A Temperature-Insensitive Third-Order Coupled-Resonator Filter for On-Chip Terabit/s Optical Interconnects

Qing Li, Siva Yegnanarayanan, Mohammad Soltani, Payam Alipour, and Ali Adibi

***Abstract*—We design and demonstrate a temperature-insensitive third-order coupled-resonator filter in the silicon-on-insulator platform for on-chip terabit/s optical interconnects. Optimum filter design enables up to 21 flat-band filter channels with more than 10 dB through-port extinction, more than 0.75-nm 3-dB bandwidth, and less than 1-dB insertion loss. By overlaying a negative thermo-optic coefficient polymer cladding on top of the silicon device, the sensitivity of the filter performance to the ambient temperature variations is significantly reduced. Moreover, through careful balancing between the dispersion of the bandwidth and the thermal property of the filter, the redundant bandwidth of filter channels due to dispersion is employed as thermal guard bands. As a result, the filter can accommodate 21 wavelength-division-multiplexing channels with data rates up to 100 Gb/s per wavelength channel while providing sufficient thermal guard bands to tolerate more than ±15 °C temperature fluctuations in the on-chip environment.**

***Index Terms*—Coupled-resonators, silicon photonics, temperature-insensitive, terabit, wavelength channels.**

I. Introduction

THE trend toward multicore architectures and chip multiprocessors requires power-efficient on-chip interconnects with terabit/s (Tb/s) capacity to facilitate information exchange among cores and the external memories [1]–[3]. A promising recent result uses wavelength-division-multiplexing (WDM) channels that are simultaneously switched and routed to provide a large aggregate bandwidth [2]. The main advantage offered by this solution is the low switching and routing power consumption. To achieve such a network, one critical element is an optical switch realized using an optical filter capable of accommodating multiple wavelength channels. Also, considering the large temperature fluctuations in a realistic on-chip environment (up to tens of degrees), the optical filter has to be temperature-insensitive [3].

Manuscript received June 14, 2010; revised September 26, 2010; accepted October 02, 2010. Date of publication October 07, 2010; date of current version November 17, 2010. This work was supported in part by the Air Force Office of Scientific Research under Contract FA9550-06-01-2003 (G. Pomrenke).

Q. Li, S. Yegnanarayanan, P. Alipour, and A. Adibi are with the School of Electrical and Computer Engineering, Georgia Institute of Technology, Atlanta, GA 30332-0250 USA (e-mail: adibi@ece.gatech.edu).

M. Soltani was with the School of Electrical and Computer Engineering, Georgia Institute of Technology, Atlanta, GA 30332 USA. He is now with the Department of Physics, Cornell University, Ithaca, NY 14853 USA.

Color versions of one or more of the figures in this letter are available online at http://ieeexplore.ieee.org.

Digital Object Identifier 10.1109/LPT.2010.2085426

In previous studies, both single- and coupled-resonator filter architectures implemented in the silicon-on-insulator (SOI) platform have been reported [3]–[5]. In [4], 20 wavelength channels were simultaneously switched using a single microring resonator. Because of the narrowband filter channels (3-dB bandwidth ∼0.1 nm), small temperature shifts can easily cause the wavelength registration problem. To solve this issue, coupled-resonator structures with large bandwidth filter channels were utilized to provide extra thermal guard bands [3], [5]. However, these coupled-resonator filters suffered from large free spectral range (FSR), which makes scalability to large WDM channel counts challenging. In addition, though a multimode interferometer coupler has been employed for a wavelength-insensitive coupling between the access waveguide and the end resonators in [3], the coupling between resonators is still evanescent, which exhibits strong dispersion over the entire wavelength range (as explained in Section II). Therefore, the overall filter performance shows strong wavelength dependence, and large distortions are observed [3].

In this letter, we show that using an evanescent coupling scheme for both the access waveguide-to-resonator and resonator-to-resonator coupling can ensure the flat-band filter response. One drawback of evanescent coupling is that the bandwidth of the filter channels increases with wavelength, resulting in redundant channel bandwidth. Here, we show that by overlaying a negative thermo-optic coefficient polymer cladding on top of the silicon device, we significantly reduce the sensitivity of the filter performance to the ambient temperature variations. Moreover, through careful balancing between the dispersion of the bandwidth and the thermal property of the filter, the redundant bandwidth of filter channels due to dispersion is employed as thermal guard bands. As a result, the filter can accommodate 21 WDM channels with data rates up to 100 gigabit/s (Gb/s) per wavelength channel while providing sufficient thermal guard bands to tolerate more than ±15 °C temperature fluctuations in the on-chip environment.

II. Device Design

The structure investigated in this letter is a symmetric third-order coupled-resonator filter, as shown in Fig. 1(a), where κ_0^2, κ_1^2 denote the power-coupling ratios between the end resonator and the access waveguide and that between the adjacent resonators. In order to minimize the impact of the strong waveguide geometric dispersion as well as the material dispersion of silicon, the FSR of the filter has to be as small as possible. Since the target 3-dB bandwidths of filter channels are on the order

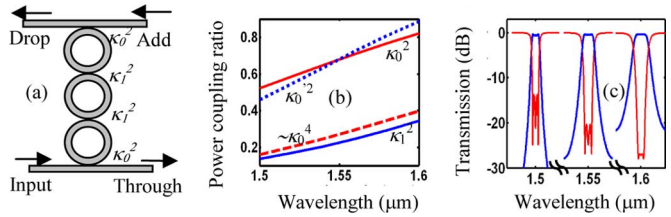

Fig. 1. (a) Schematic of the third-order filter; (b) power-coupling ratios of the synchronous parallel waveguide couplers with different gaps and coupling lengths: κ_0^2 (gap 160 nm, length 4.4 μm), $\kappa_0'^2$ (gap 300 nm, length 10.2 μm), and κ_1^2 (gap 300 nm, length 5.2 μm); (c) three simulated filter channel responses with power-coupling ratios κ_0^2 and κ_1^2 provided in (b).

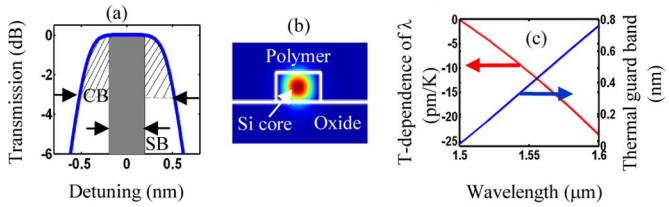

Fig. 2. (a) Illustration of extra channel bandwidth as thermal guard band (hatched region); CB: filter channel bandwidth; SB: signal information bandwidth. (b) Cross section of the waveguide structure on an SOI substrate with a polymer cladding. (c) The left axis shows the wavelength temperature dependence of the filter, and the right axis shows the thermal guard band for 100-Gb/s wavelength channels.

of 1 nm to accommodate wideband wavelength channels (e.g., 100 Gb/s), an FSR around 5 nm is empirically found to be appropriate to provide the necessary bandwidth and adequate channel isolation. To obtain a flat-band response, κ_0^2 and κ_1^2 have to satisfy certain relationships. For example, in the narrowband filter design, $\kappa_1^2/\kappa_0^4 \approx 1/8$ is required, while in the wideband filter design, the exact ratio of κ_1^2/κ_0^4 may be different [5]. Therefore, for flat-band design, κ_0^4 and κ_1^2 should follow a similar wavelength-dispersion curve.

In this work, resonators and waveguides are evanescently coupled to each other. The design approach consists of two aspects, the first being broadband coupling engineering and the second being temperature-insensitive design. Initially, the waveguide dimensions are optimized to fine tune the thermal property of the filter. We use a waveguide with a height of 144 nm and a width of 425 nm covered with a top polymer cladding to achieve an athermal response exactly at 1.5 μm for the fundamental transverse-electric mode. The choice of this wavelength for the athermal operation will be elaborated on later. Since we are targeting multiple filter channels ($\sim$20) over a wide wavelength range ($\sim$100 nm), the resonator's coupling to the access waveguides and the adjacent resonators needs to be optimized to achieve wideband coupling performance. In this regard, a microring performs significantly better than a racetrack due to its effective shorter coupling length under fixed FSR and power coupling ratio. While a detailed comparison could be performed through three-dimensional finite-difference time-domain (FDTD) simulations, here we adopt a simpler approach where the coupling region of two coupled structures is modeled by a parallel waveguide coupler with the same gap and an equivalent coupling length [6]. Fig. 1(b) shows the simulation results for the dispersion of the power coupling ratios of a synchronous parallel waveguide coupler (with the mentioned waveguide dimension) for different values of gaps and coupling lengths. The upper two curves correspond to couplers with identical power coupling ratios at $\lambda = 1.55$ μm, but the one with a shorter coupling length exhibits less dispersion over the wavelength range 1.5–1.6 μm. This observation leads us to use microrings with a radius of 21 μm (instead of racetracks) for the filter design. Following the procedure outlined in [5], which uses the synchronous parallel-coupler model, the waveguide-resonator and resonator-resonator gaps are found to be 160 and 300 nm, resulting in an equivalent coupling length of 4.4 and 5.2 μm, respectively. κ_0^2 and κ_1^2 are shown accordingly in Fig. 1(b) by the upper solid line and the lower solid line, respectively. The condition for a flat-band response is also verified in Fig. 1(b), where κ_0^4 shows a similar dispersion compared to κ_1^2. Using these parameters for the device, the overall filter response is obtained through a rigorous matrix analysis [5]. In Fig. 1(c), we show three such filter channels around 1.5, 1.55, and 1.6 μm. From Fig. 1(c), we observe that 1) filter responses are reasonably good, and flat-band filter channels exhibit more than 15-dB extinction in the through port and more than 20-dB out-of-band rejection in the drop port; 2) the 3-dB bandwidth increases from 0.75 nm at $\lambda = 1.5$ μm to 1.5 nm at $\lambda = 1.6$ μm, primarily due to the dispersion impacting κ_0^2 and κ_1^2, as seen in Fig. 1(b); 3) the bandwidth of the filter channels increases with wavelength, and the finesse of the filter decreases; consequently, the out-of-band rejection becomes smaller (more than 30 dB at 1.5 μm and only 20 dB at 1.6 μm); 4) the through-port responses are improved at longer wavelengths, indicating a better impedance match among coupled resonators and the end waveguides.

Following efficient broadband coupling engineering, we proceed to the second aspect of the design for temperature-insensitive operation. Fig. 2(a) shows the concept of thermal guard band. The solid curve shows the optical filter passband response, and the solid filled rectangle shows the input optical signal information bandwidth, which can be as large as the 3-dB bandwidth of the filter channel [1], [4]. The remaining spectral portion shown by the hatched region illustrates the available thermal guard band. Our design for the temperature-insensitive filter centers on the complete athermal operating point at the wavelength channel with the smallest bandwidth (in our case this is at $\lambda = 1.5$ μm). This ensures that throughout the entire working wavelength range, the overall available thermal guard band is optimally utilized. To achieve this, we overlay the silicon device with an acrylate polymer [see Fig. 2(b)] with a refractive index close to the oxide ($n = 1.45$) and a large negative thermal-optic coefficient of -4.5×10^{-4}/K [7]. To increase the overlap between the optical field and the polymer cladding, the silicon device layer is thinned to 144 nm, and the required waveguide width is calculated to be 425 nm for complete athermal operation at $\lambda = 1.5$ μm. Fig. 2(c) shows the simulated temperature dependence of the filter over the entire working wavelength range, which increases from 0 pm/K at $\lambda = 1.5$ μm to 23 pm/K at $\lambda = 1.6$ μm. To illustrate the operation of our filter, we consider the following scenario: If the filter is used for wavelength channels modulated at 100-Gb/s data rate, at $\lambda = 1.5$ μm, the available guard bandwidth is small (3-dB bandwidth 0.75 nm), but due to the centering of athermal operation to

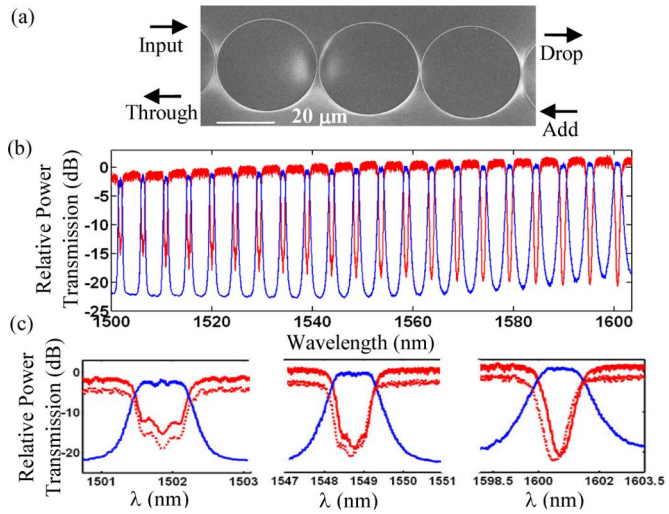

Fig. 3. (a) Scanning-electron micrograph of the fabricated filter; (b) measured transmission responses for the fabricated filter; (c) detailed measured spectra of three representative channels. The dotted lines show the through-port responses after a 10 °C temperature rise.

this wavelength, the filter channel shifts very little with the temperature. At the other end of the filter operation, at $\lambda = 1.6\ \mu$m, the filter channel has a relatively large temperature dependence of -23 pm/K, but it also has a large available guard band of 0.75 nm (3-dB bandwidth 1.5 nm), thus allowing for ± 15 °C temperature fluctuations [see Fig. 2(c)]. For lower data rate signals, even larger temperature fluctuations can be tolerated.

III. Device Fabrication and Experimental Results

The device is fabricated on an SOI wafer with a 144-nm-thick silicon layer on top of a 3-μm-thick buried oxide substrate. The devices are patterned using a JBX-9300FS electron beam lithography system, followed by plasma etching and spin coating the polymer cladding on the top surface. Details of fabrication and characterization are referred to in [5] and [7].

Fig. 3(a) shows the scanning electron micrograph of the fabricated device, and Fig. 3(b) shows its measured transmission. Twenty-one filter channels with more than 10-dB through-port extinction and 20-dB drop-port out-of-band rejection are obtained. The insertion loss of the filter can be estimated by the difference between the maxima of the through and drop ports to be less than 1 dB. In Fig. 3(c), we show three representative filter channels at wavelengths 1.5, 1.55, and 1.6 μm, respectively. Compared with the simulation results shown in Fig. 1(c), the 3-dB bandwidths agree well with the design, being 0.75, 1.12, and 1.5 nm for the corresponding channels. The out-of-band rejections in the drop port at lower wavelengths, which are predicted to be higher in Fig. 1(c) ($>$25 dB), are limited to 22 dB. This deviation is believed to arise from the limited dynamic range of our measurement setup, which has a relatively large noise floor. The reduction of the out-of-band rejections at longer wavelengths, as seen for the filter channels near $\lambda = 1.6\ \mu$m, is expected and is in agreement with the theory. The through-port responses are a little degraded from the design, as the extinction drops to 10 dB at $\lambda = 1.5\ \mu$m instead of 15 dB, and the shape is also deformed. This is because the through-port responses are very sensitive to the resonance frequency mismatches between the coupled resonators [6], which can be easily caused by the imperfect fabrication processes.

The temperature behavior of the filter is also tested by heating the device using a thermal stage and measuring the transmission [7]. In Fig. 3(c), the corresponding through-port responses after a 10 °C temperature rise are shown by dotted lines (deliberately moved down 3 dB for better illustration). We can verify that the filter is indeed athermal at $\lambda = 1.5\ \mu$m and has wavelength-temperature dependencies of -12 and -25 pm/K at wavelengths 1.55 and 1.6 μm, respectively. This is a significant improvement compared to conventional unclad filters ($\sim$70 pm/K) [3].

In conclusion, we have designed and demonstrated a third-order flat-band filter that can accommodate 21 WDM channels with data rates up to 100 Gb/s per wavelength channel, totaling up to a 2.1-Tb/s aggregate capacity. The filter can tolerate more than 30° temperature fluctuations in the on-chip environment. The footprint of the filter is less than 0.005 mm^2. In the future, we envision the addition of active switching functionality to the filter through carrier injection (either all-optically or electrically), and a high-performance switch with a switching speed on the order of nanoseconds is expected [3]. Such a compact, wideband, temperature-insensitive optical switch would be a critical building block in future on-chip optical networks.

References

[1] K. Bergman, "Silicon photonic on-chip optical interconnection networks," in *Proc. Frontiers in Nanophotonics and Plasmonics*, Guaruja, Brazil, Nov. 2007.

[2] A. Shacham, K. Bergman, and L. P. Carloni, "Photonic networks-on-chip for future generations of chip multiprocessors," *IEEE Trans. Comput.*, vol. 57, no. 9, pp. 1246–1260, Sep. 2008.

[3] Y. Vlasov, W. M. J. Green, and F. Xia, "High-throughput silicon nanophotonic wavelength-insensitive switch for on-chip optical networks," *Nature Photon.*, vol. 2, pp. 242–246, Apr. 2008.

[4] B. G. Lee, A. Biberman, P. Dong, M. Lipson, and K. Bergman, "All-Optical comb switch for multiwavelength message routing in silicon photonic networks," *IEEE Photon. Technol. Lett.*, vol. 20, no. 10, pp. 767–769, May 2008.

[5] Q. Li, M. Soltani, S. Yegnanarayanan, and A. Adibi, "Design and demonstration of compact, wide bandwidth coupled-resonator filters on a silicon-on-insulator platform," *Opt. Express*, vol. 17, no. 4, pp. 2247–2254, Feb. 2009.

[6] Q. Li, M. Soltani, A. H. Atabaki, S. Yegnanarayanan, and A. Adibi, "Quantitative modeling of coupling-induced resonance frequency shift in microring resonators," *Opt. Express*, vol. 17, no. 26, pp. 23474–23487, Dec. 2009.

[7] P. Alipour, E. S. Hosseini, A. A. Eftekhar, B. Momeni, and A. Adibi, "Athermal performance in high-Q polymer-clad silicon microdisk resonators," *Opt. Lett.*, vol. 35, no. 20, pp. 3462–3464, Oct. 2010.